Phys. Status Solidi C 7, No. 1, 64–67 (2010) / DOI 10.1002/pssc.200982612

physica status solidi c
www.pss-c.com
current topics in solid state physics

Inter- and intrasubband spectroscopy of cubic AlN/GaN superlattices grown by molecular beam epitaxy on 3C-SiC

C. Mietze[*,1], E. A. DeCuir, Jr.[2], M. O. Manasreh[2], K. Lischka[1], and D. J. As[,1]**

[1] Department of Physics, University of Paderborn, Warburger Str. 100, D-33095 Paderborn, Germany
[2] Department of Electrical Engineering, University of Arkansas, 3217 Bell Engineering Center, Fayetteville, Arkansas 72701, USA

Received 19 June 2009, accepted 26 September 2009
Published online 9 December 2009

PACS 61.05.cp, 78.30.Fs, 78.55.Cr, 78.67.Pt, 81.05.Ea, 81.15.Hi

* Corresponding author: e-mail cmietze@mail.upb.de
** e-mail: d.as@uni-paderborn.de

We report the growth of cubic GaN/AlN multi quantum well (MQW) structures by plasma-assisted molecular beam epitaxy on 10 µm thick 3C-SiC on top of 300 µm silicon. The samples consist of 115 nm thick GaN buffer and 20 periods of GaN/AlN active regions. The thickness of the AlN barrier is 1.48 nm for all samples, while the thickness of the GaN quantum wells varies between 1.36 nm-2.94 nm. The growth was observed by in-situ reflection high energy electron diffraction (RHEED). The structural properties of our samples were studied by high resolution x-ray diffraction (HRXRD). Several peaks in the HRXRD spectra reveal a high structural perfection of the MQW region. Clear evidence for inter- and intrasubband transitions was observed in photoluminescence (PL) and infrared absorbance spectra measured at temperatures between 2 K and 300 K.

1 Introduction Intrasubband transitions (ISBT) in superlattices (SL) or multiple quantum wells (MQW) form the basis for quantum well infrared photodetectors and quantum cascade lasers [1]. Due to the wide band gaps and large band offsets between AlN and GaN this group of III-nitrides offers the possibility of fabricating multi quantum well structures with intrasubband transitions in the technologically important 1.3-1.55 µm infrared spectral range. However, a major challenge for the design of GaN/AlN devices is the presence of strong intrinsic piezoelectric and pyroelectric fields at each hetero-interface. These fields are generated by sheet charges at each hetero-interface. Though, these built-in fields are not present in MQWs with nonpolar hexagonal [1] and cubic crystal structure [2]. The growth of metastable cubic GaN/AlN multi quantum wells on (001) oriented substrates eliminates the distracting internal fields [3] and allows easier design of superlattice structures with different quantum well widths for intrasubband transitions.

2 Experimental All quantum structures were grown at $T_{substrate}$=720 °C on 10 µm thick 3C-SiC on top of 300 µm Si (NovaSiC) by plasma assisted molecular beam epitaxy (MBE). A 115 nm thick cubic GaN (c-GaN) buffer layer was deposited on the 3C-SiC substrate. Growth was controlled by Reflection High Energy Electron Diffraction (RHEED) [4]. Subsequently, a 20 period superlattice (SL) consisting of GaN/AlN was grown. The thickness of the AlN barriers was 1.48 nm and the well width of the GaN quantum wells was varied between 1.36 nm and 2.96 nm, respectively. The SL was followed by another 115 nm thick c-GaN cap layer. During deposition of the SL, growth was interrupted for 20 s after each layer. This procedure allowed excess metal to evaporate from the surface. The structural properties of the samples produced

in this way were characterized by high resolution x-ray diffraction (HRXRD). From the diffraction profiles lattice parameter and structural quality of the superlattice samples could be obtained. Reciprocal space maps (RSM) of $(\overline{1}\overline{1}3)$ reflex were measured to reveal if the layers are pseudomorphically strained or relaxed.

The surface roughness was controlled after growth using atomic force microscopy (AFM).

Photoluminescence (PL) measurements were recorded, using a HeCd Laser with an emission wavelength of 325 nm (3.81 eV) as excitation source. An interference filter suppressed the plasma lines. The spotsize on the sample was about 1 mm^2 and the output power was about 4 mW. A Spex 270m monochromator combined with a GaAs photomultiplier and a Hamamatsu C3866 photon counter was used to detect emitted light of the superlattice samples. A computer system served for data collection and visualisation. During the measurement the samples were mounted in a He bath cryostat which allowed PL measurements in the temperature range of 2-300 K. PL spectra of superlattices with different QW-widths and constant barrier widths were recorded at 300 K and 2 K. From the PL data the transition between the lowest conduction band subband and the highest valence band subband could be observed and the transition energy could be calculated.

For optical absorption measurements a Bruker Fourier-transform 125HR spectrometer, consisting of a quartz-halogen light source, an InSb cooled detector, and a calcium fluoride beam splitter was used. This configuration makes measurements in the spectral range of 1-3 µm possible. The samples were cut into waveguides with 45° facets by lapping to enable multiple passes of incident light through the superlattice.

The band structure and bound state energy levels were calculated using a self-consistent Poisson-Schrödinger model (1D Poisson) [5]. Energy differences between the bound states were obtained from the well and barrier widths. Theoretical values for intersubband transitions and intrasubband transitions were compared to the experimental data of PL and infrared absorption measurements.

3 Results and discussion

3.1 RHEED Growth of metastable cubic GaN/AlN layers is a superior challenge because of the narrow growth parameter window [6]. The growth parameters like substrate temperature and temperatures of the effusion cells have to be controlled carefully to permit structurally perfect superlattices. The most important tool to observe growth is in-situ RHEED. It has been shown c-GaN layers with the best structural quality are grown under one monolayer Ga coverage on the surface [4]. A typical timescan of RHEED intensity during growth of one period AlN/GaN superlattice is shown in Fig.1. The coloured areas denote the growth of the different layers. In between the growth periods growth was interrupted for 20 s. After the growth of the GaN layer RHEED intensity rises due to evaporation of excess metal. During growth of AlN clear RHEED-oscillations can be observed which indicate step flow growth of the layer. From the oscillation period a growth rate of 0.13 ML/s was determined. The AlN layers were grown under nitrogen-rich conditions. During c-GaN growth no RHEED-oscillations can be observed due to gallium-rich growth conditions. Growth rate of c-GaN was investigated by post growth thickness measurements and was estimated to be 0.14 ML/s.

3.2 X-ray and AFM From an asymmetrical reciprocal space map of the $(\overline{1}\overline{1}3)$ reflex of the superlattices grown on c-GaN one can obtain if the superlattices are grown pseudomorphic or relaxed on the buffer layer. The lattice

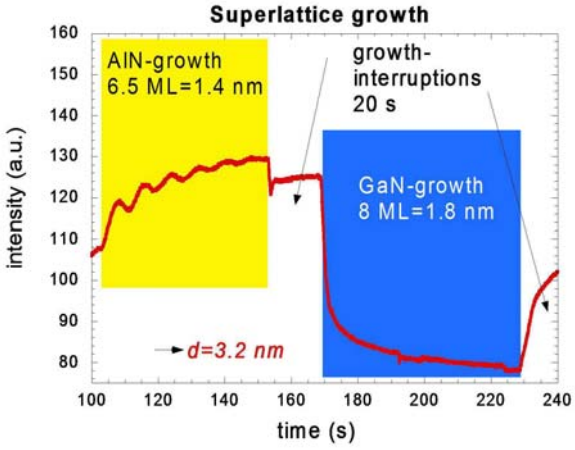

Figure 1 RHEED intensity timescan of one period of superlattice growth. Thickness of AlN barrier is determined to be 1.4 nm and GaN quantum well width is calculated from growth rate to be 1.8 nm.

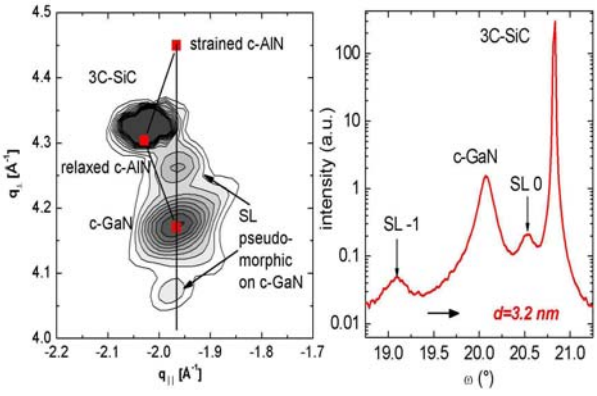

Figure 2 Reciprocal space map of $(\overline{1}\overline{1}3)$ reflex (left hand) and HRXRD ω-2θ scan of (002) reflex of a 20 period 1.8 nm GaN/1.5 nm AlN superlattice sample (right hand).

period of the superlattice samples was determined from ω-2θ scans using a high resolution x-ray diffractometer. In Figure 2 an asymmetrical reciprocal space map of the $(\overline{1}13)$ reflex (left) and an ω-2θ scan of the (002) reflex of a superlattice (right) consisting of 20 periods of 1.81 nm GaN wells and 1.48 nm AlN barriers are shown. The positions of the superlattice reflexes in the reciprocal space map (left side of Fig. 2) reveal that the superlattice is pseudomorphically strained on the c-GaN. The ω-2θ scan on the right side of Fig. 2 shows two additional peaks beyond the c-GaN peak and the 3C-SiC peak. These two peaks correspond to the grown superlattice. The periodicity of the superlattice can be calculated from the positions of the superlattice peaks [7]. The superlattice periodicity is estimated to be 3.2 nm which is in good agreement with the value of 3.2 nm estimated from RHEED timescan in Fig. 1. Using atomic force microscopy the surface RMS roughness of the superlattice samples was estimated for areas of 5x5 μm^2. The values vary between 2.0 nm and 4.0 nm and are in the same order of the best values reported for bulk c-GaN [4]. These values also give proof of the high quality of the samples.

3.3 Intersubband transitions The room temperature photoluminescence spectra for three different superlattice samples with GaN quantum well widths of 2.0 nm, 1.8 nm, and 1.6 nm, respectively are plotted in Fig. 3. Clear luminescence corresponding to the superlattice can be observed in addition to the luminescence of bulk c-GaN. For better overview the spectra were normalized on the superlattice peak. With descending well width the superlattice peak shifts to higher energies. The luminescence can be related to the transition from the lowest conduction band subband to the highest valence band subband. The fact, that luminescence of the superlattice can be observed gives on the one hand proof for the high structural quality of the samples and on the other hand proof for the presence of minibands. PL spectra for the same superlattice samples at $T = 2$ K are plotted in Fig. 4. Clear luminescence corresponding to the superlattices can be observed at $T = 2$ K too. Compared to room temperature photoluminescence the superlattice peaks shift to higher energies due to the larger band gap of c-GaN at low temperatures. For the sample with 2.0 nm GaN QWs two separate peaks are observed. The energy difference of 0.04 eV between the peaks can be explained by a width fluctuation of the quantum well of one monolayer. For bulk c-GaN the well known luminescence of the free exciton (X) and the donor acceptor transition (D^0A^0) at low temperatures is observed [8].

The transition energy of the superlattice photoluminescence is compared to theoretical values for the intersubband transition, calculated with a self-sonsistent Poisson-

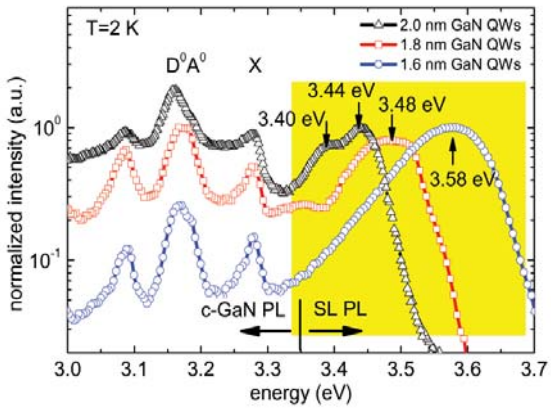

Figure 4 Photoluminescence spectra of 20 period 2.0 nm, 1.8 nm, 1.6 nm GaN/1.5 nm AlN superlattice samples at T=2 K.

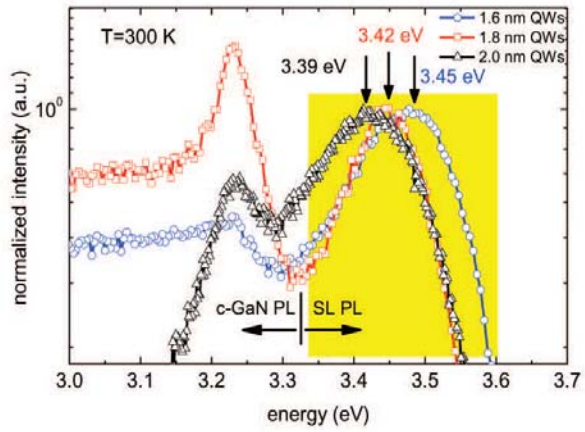

Figure 3 Photoluminescence spectra of 20 period 2.0 nm, 1.8 nm, 1.6 nm GaN/1.5 nm AlN superlattice samples at T=300 K.

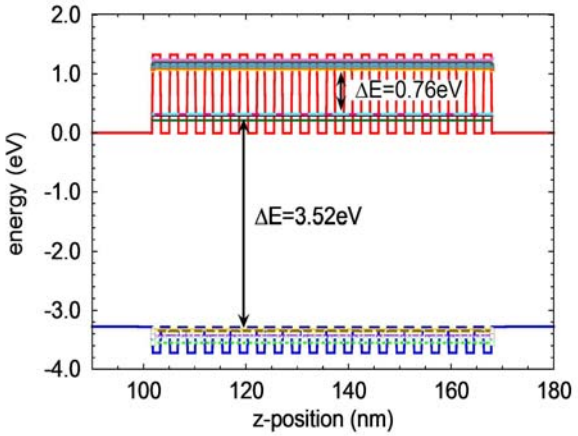

Figure 5 Simulated band structure of a 20 period 1.8 nm GaN/1.5 nm AlN superlattice sample using a self-consistent Poisson-Schrödinger model (1D Poisson).

Schrödinger model. Figure 5 shows the calculated band structure for a 20 period superlattice consisting of 1.81 nm GaN/1.48 nm AlN layers at T=2 K. The intersubband transition which could be observed by photoluminescence and the intrasubband transition are both inscribed in the diagram. For the theoretical calculations a conduction band to valence band offset ratio of 70:30 was assumed. The other parameters used are given in Table 1.

The deviation of 0.04 eV between the theoretical value of 3.52 eV and the experimental value (3.48 eV) for the intersubband transition is due to width fluctuations of the GaN and AlN layers. These may be caused by fluctuations of the nitrogen flux or an inhomogeneous heat in coupling into the wafer during growth. The c-GaN layers are grown under metal rich conditions, so fluctuations in the atomar N-flux lead to fluctuations of the QW thickness. Higher temperatures lead to higher material desorption, leading to thinner layers and vice versa. Thus inhomogeneous heat in coupling influences the thickness of all layers.

3.4 Intrasubband transitions The infrared absorbance spectra of the intrasubband transitions in three superlattice samples are shown in Fig. 6. The absorbance is defined as the product of the absorption coefficient (α) and the thickness of the GaN quantum wells (L_w). Due to the small barrier width the localized wave functions in neighbouring quantum wells overlap, leading to the formation of mini-bands. Absorbance in the spectral range of 1.6 µm-2 µm could be observed. The results of the absorbance measurements (Fig. 6) are also in good agreement with the theoretical values (Fig. 5). For example there is only a deviation of 30 meV between the experimental value of 0.73 eV and the theoretical value of 0.76 eV for the 1.8 nm GaN/1.5 nm AlN sample which can be explained by width fluctuations of the c-GaN quantum wells. For the sample with 1.8 nm quantum wells oscillations of the absorbance can be observed. These are interference fringes of the 10 µm thick SiC layer. The absence of the oscillations in the other spectra may be connected to different in coupling into the waveguide.

Table 1 Parameters used for band structure simulation.

Parameter	c-AlN	c-GaN
E_{gap}	5.2 eV	3.2 eV
m^*_{hh}/m_0	1.2	0.8
m^*_{lh}/m_0	0.33	0.18
m^*_e/m_0	0.19	0.15

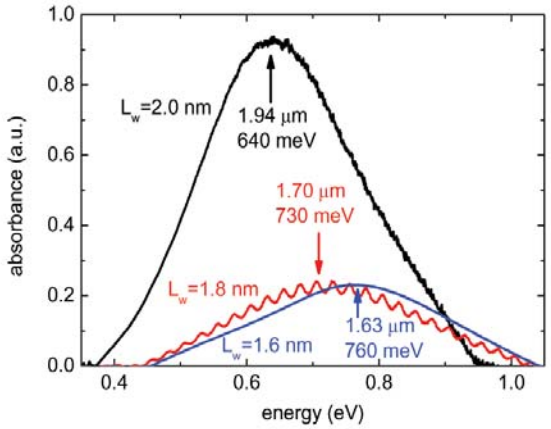

Figure 6 Absorbance spectra of three different superlattice samples, consisting of 20 period 1.58 nm GaN, 1.6 nm GaN and 2.0 nm GaN/1.5 nm AlN superlattices.

4 Conclusion Nonpolar zincblende GaN/AlN superlattices with intersubband transitions in the range of 3.4 eV-3.6 eV and intrasubband transitions in the spectral range of 640 meV-760 meV were fabricated by plasma assisted molecular beam epitaxy. So the intrasubband transitions are in the technologically interesting region of 1.6-2.0 µm. The thicknesses of the single layers were observed in-situ by RHEED and the lattice period was confirmed by HRXRD measurements. High quality of the samples was approved and the existance of mini-bands was shown by clear photoluminescence. Intersubband transitions were observed at $T = 300$ K and $T = 2$ K. Room temperature infrared absorbance due to intrasubband transitions was observed near the technological important 1.55 µm spectral region. The experimental results were comfirmed by theoretical calculations using a self-consistent Poisson-Schrödinger model which showed good agreement with the experimental results.

Acknowledgements The support by Deutsche Forschungsgemeinschaft, Project No. As 107/4-1 is acknowledged.

References

[1] G. Gmachl and H.M. Ng, Electron. Lett. **39**, 567 (2003).
[2] E.A. DeCuir, Jr., E. Fred, M.O. Manasreh, J. Schörmann, D.J. As, and K. Lischka, Appl. Phys. Lett. **91**, 041911 (2007).
[3] J. Schörmann, S. Potthast, D.J. As, and K. Lischka, Appl. Phys. Lett. **89**, 131910 (2006).
[4] J. Schörmann, S. Potthast, D.J. As, and K. Lischka, Appl. Phys. Lett. **90**, 041918 (2007).
[5] I.H. Tan, G.L. Snider, L.D. Chang, and E.L. Hu, J. Appl. Phys. **68**, 4071 (1990).
[6] D.J. As, S. Potthast, J. Schörmann, S.F. Li, K. Lischka, H. Nagasawa, and M. Abe, Mater. Sci. Forum **527-529**, 1489 (2006).
[7] J. Schörmann, S. Potthast, M. Schnietz, S. Li, D.J. As, and K. Lischka, Phys. Status Solidi C **5**, No 6, 2092 (2008).
[8] D.J. As, F. Schmilgus, C. Wang, B. Schöttker, D. Schikora, and K. Lischka, Appl. Phys. Lett. **70**, 1311 (1997).